Honeycomb Porous Films Prepared from Porphyrin-Cored Star Polymers: Submicrometer Pores Induced by Transition of Monolayer into Multilayer Structures

ARTICLE *in* THE JOURNAL OF PHYSICAL CHEMISTRY C · MARCH 2013

Impact Factor: 4.77 · DOI: 10.1021/jp311439p

4 AUTHORS, INCLUDING:

Liangwei Zhu
Zhejiang University
11 PUBLICATIONS **122** CITATIONS
SEE PROFILE

Zhi-Kang Xu
Zhejiang University
249 PUBLICATIONS **6,163** CITATIONS
SEE PROFILE

THE JOURNAL OF PHYSICAL CHEMISTRY C

Article

pubs.acs.org/JPCC

Honeycomb Porous Films Prepared from Porphyrin-Cored Star Polymers: Submicrometer Pores Induced by Transition of Monolayer into Multilayer Structures

Liang-Wei Zhu, Ling-Shu Wan,* Jing Jin, and Zhi-Kang Xu

MOE Key Laboratory of Macromolecular Synthesis and Functionalization, Department of Polymer Science and Engineering, Zhejiang University, Hangzhou 310027, P. R. China

Supporting Information

ABSTRACT: Honeycomb porous films prepared by the breath figure method show great potential in fields such as templating, separation, microanalysis, and superhydrophobic materials. This method is of significant simplicity but generally generates films with pores larger than 1 μm. Here we report an approach to formation of films with pore diameter as small as about 240 nm, which is based on the transition of monolayer into multilayer structures. Porphyrin-cored star polymers poly(styrene-*block*-2-hydroxyethyl methacrylate) having on average only 1−2 hydrophilic monomer units were synthesized by atom transfer radical polymerization (ATRP) and used for preparing honeycomb films. We investigated the effects of polymer structure and concentration on the pore diameter and film morphology. A tentative mechanism for the formation of multilayer structures was proposed and experimentally verified by in situ observing the breath figure process and measuring the glass transition temperature of the stars using differential scanning calorimetry (DSC). This work is helpful in understanding the mechanism of the breath figure method and preparing honeycomb films with submicrometer-sized pores which show perspectives as advanced microfiltration membranes.

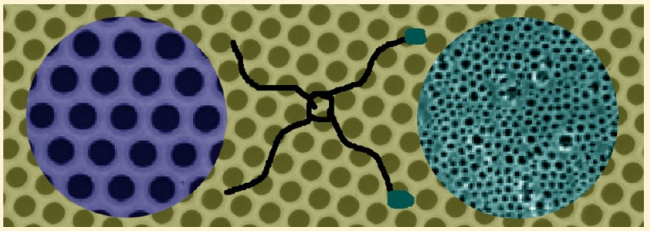

INTRODUCTION

Ordered structures exist in nature widely. For example, the siliceous cell wall of a diatom is a honeycomb consisting of the vertical areolae walls arranged in hexagons; the elaborate patterns of diatom are related to not only the bulk properties such as mechanical strength and density but also the functionalities such as photosynthesis.[1] Ordered structures can be artificially fabricated by technology of microfabrication or self-assembly.[2] Since being invented by Wadawski and co-workers in 1994,[3] the breath figure method has showed great potential in preparing honeycomb films which are useful as microarrays of biomolecules[4−7] or particles,[8−14] patterning templates,[15,16] superhydrophobic surfaces,[17] biomaterials,[18−21] sensing[22] and photoelectronic materials,[23−28] microcontainer or reactor,[29,30] and separation membranes.[31,32]

Control over the pore size of honeycomb films is very important. In the breath figure process, the foggy array of water droplets is induced by solvent evaporative cooling and serves as sacrificial templates for spherical pores, leaving a honeycomb patterned porous film after further evaporation of the water droplets. The pores are shaped by the water droplets. It has been reported that the pore size can be influenced by various factors such as the precipitation of polymers, the rate of solvent evaporation, and the rate of water condensation and growth. The complexity of the process with its manifold influences does not readily allow an absolute prediction or control of the pore size, and even the developed empirical relationships only work well in certain systems.[33] Therefore, although the smallest theoretical size of a water droplet at room temperature has been reported to be 10 nm,[34] the breath figure method produces films with pore sizes ranging from 1 to 10 μm in most cases.[35−38] As far as we know, only Stenzel, Shimomura, and Bolognesi and their co-workers ever reported films that have pore sizes between 100 and 400 nm.[17,39−41] However, for example, Yabu and Shimomura observed pores of about 100 nm, but they were only located in the very small edge area (tens of micrometers) of the film where the solvent evaporates fast.[17] Up to now, how to fabricate honeycomb films with submicrometer-sized pores by the breath figure method remains a challenge.

In this work, we found that polystyrene (PS) stars having a very short hydrophilic block show significantly different film-forming behaviors when compared with PS stars without hydrophilic teminal groups or blocks. We therefore proposed a strategy to fabricate films with submicrometer-sized pores in the whole film area, which is based on the formation of multilayer structures. The structure may be induced by both long solidifying time of the polymer solution, which allows repeated migration of stabilized water droplets to close to the three-phase line, and fast precipitation of polymers, which limits the growth of condensed water droplets.[33,35] This strategy opens a new route for facilely preparing honeycomb films with

Received: November 20, 2012
Revised: January 30, 2013
Published: March 4, 2013

   dx.doi.org/10.1021/jp311439p | *J. Phys. Chem. C* 2013, 117, 6185−6194

submicrometer-sized pores and is helpful in further understanding the mechanism of the breath figure method. In addition, as the films were prepared from star polymers with porphyrin cores, they are one kind of fluorescent film material.

EXPERIMENTAL METHODS

Materials. Styrene (St) and anisole were obtained from Sinopharm Chemical Reagent Co. and distilled under reduced pressure before use. 2-Hydroxyethyl methacrylate (HEMA, 97%, Aldrich) was purified through an alumina column. 2-Bromoisobutyryl bromide (BIBB, 98%, Aldrich) was used as received. *N*,*N*,*N*′,*N*′-Pentamethyldiethylenetriamine (PMDETA, Aldrich) and triethylamine were distilled from calcium hydride; dichloromethane was distilled from phosphorus pentoxide; and all of them were stored at room temperature in a desiccator. Copper(I) bromide (CuBr) was stirred in glacial acetic acid overnight, filtered, and washed with absolute ethanol under an argon blanket. The compound was dried under reduced pressure at 60 °C overnight. Deuterated chloroform ($CDCl_3$, 99.9%) and deuterated dimethyl sulfoxide (DMSO-d_6, 99.9%) were purchased from Sigma. Water used in all experiments was deionized. All other chemicals were analytical grade and used as received.

Methods. Proton nuclear magnetic resonance (^{1}H NMR) spectra were recorded on a Bruker (Advance DMX500) NMR instrument with tetramethylsilane (TMS) as the internal standard, using $CDCl_3$ or DMSO-d_6 as the solvent at room temperature. Fourier transform infrared (FTIR) spectra were collected on a Nicolet FTIR/Nexus 470 spectrometer. Thirty-two scans were taken for each spectrum at a nominal resolution of 1 cm^{-1}. Molecular weight and molecular weight distribution were measured by a PL 220 GPC instrument at 25 °C, which was equipped with a Waters 510 HPLC pump, three Waters Ultrastyragel columns (500, 103, and 105 Å), and a Waters 410 DRI detector. THF was used as the eluent at a flow rate of 1.0 mL/min. The calibration of the molecular weights was based on polystyrene standards.

UV−vis spectra of the solutions were recorded with a Shimadzu UV 2450 spectrophotometer (Shimadzu, Japan). UV−vis spectra of the films were obtained using a Shimadzu integrating sphere accessory assembled in the above-mentioned spectrophotometer. Fluorescence emission spectra of the solutions were conducted on Shimadzu RF-3510 PC fluorescence spectrophotometer. Fluorescence emission spectra of the films were conducted on the same machine with an accessory for solid sample. Fluorescence microscopy image of the films was obtained on a fluorescence microscope (Nikon Ti−U).

The glass transition temperature (T_g) of the star polymers was measured by differential scanning calorimeter (DSC) on a TA Q200 DSC instrument under nitrogen atmosphere. $TPP(PS)_4$ (8.81 mg), $TPP(PS_{37}$-*b*-$PHEMA_{1.4})_4$ (9.72 mg), or $TPP(PS_{37}$-*b*-$PHEMA_7)_4$ (9.39 mg) was sealed in an aluminum sample crucible under nitrogen protection. Then the DSC scan was recorded at a heating rate of 20 °C/min from 40 to 150 °C, followed by immediately cooling from 150 to 40 °C at 20 °C/min, then again heated from 40 to 150 °C at 20 °C/min. The second heating cycle was recorded for T_g measurement.

A field emission scanning electron microscope (FESEM, Hitachi S4800 and Sirion-100, FEI) was used to observe the surface morphology of films after being sputtered with gold using an ion sputter JFC-1100. Pore diameter was analyzed using ImageJ (v1.42q, by Wayne Rasband). Height images were recorded by atomic force microscopy (AFM, Nanoscope Multimode IIIA) under tapping conditions. The radius of curvature of the tip used was ∼5 nm. The scanning parameters are as follows: scanning rate is 1.00 Hz, scanning size is 10 μm, and the line direction is retrace scanning.

Synthesis of THPP. *meso*-Tetrakis(4-hydroxylphenyl) porphyrin (THPP) was synthesized by the Adler−Longo method. Briefly, parahydroxybenzaldehyde (1.83 g, 15 mmol) and propanoic acid (40 mL) were added to a 250 mL three-necked bottle equipped with a condenser and a constant pressure drop funnel and heated to 140 °C. Propionic acid (10 mL) including 1.05 g of pyrrole (15 mmol) was then added in 30 min under the state of stirring. Ethanol (40 mL) was added after the reaction proceeded for another 2 h followed by cooling to room temperature. The solution was kept in a refrigerator for 1 h, and the final suspension was filtered and successively washed with the mixture of propanoic acid and ethanol (1:1, v/v), chloroform, and ethanol. The solvent of the filtrate was removed under reduced pressure by rotary evaporation to produce purple powder. The powder was further purified by column chromatography using ethyl acetate as the eluent. The resulted powder was dried in a vacuum oven overnight to achieve the final product. As a result, THPP was obtained with a yield of about 4.5%. ^{1}H NMR (500 MHz, DMSO-d_6): δ (ppm) −2.82 (H, NH), 7.2 (8H, ortho-H phenyls), 8.0 (8H, meta-H phenyls), 8.86 (H, pyrrole β-H), 10 (H, OH). IR: ν (cm^{-1}) 1608, 1502, 1350, 1172, 966, 802, 731.

Conversion of THPP into ATRP Initiator, TPPBr. The synthesis of atom transfer radical polymerization (ATRP) initiator, TPPBr, was performed as follows.[42] Dichloromethane (50 mL), THPP (200 mg, 0.29 mmol), and triethylamine (0.5 mL) were added to a 250 mL three-necked bottle equipped with a constant pressure drop funnel. The bottle was purged with nitrogen for 10 min and cooled in an ice−water bath. Dichloromethane (10 mL) containing BIBB (1.6 g, 7.0 mmol) was placed in the constant pressure drop funnel and added dropwise to the reaction bottle. The reaction was kept for 2 h in the ice−water bath followed by 16 h at room temperature. The resulting solution was extracted by 1% NaOH aqueous solution, and the dark red solution was collected. Rotary evaporation of the solution results in purple powder, which was further purified by column chromatography using dichloromethane as the eluent. The resulting powder was dried in a vacuum oven overnight to achieve the final product TPPBr with a yield of about 77.5%. ^{1}H NMR (500 MHz, $CDCl_3$): δ (ppm) −2.82 (H, NH), 2.1 (3H, CH_3), 7.45 (8H, ortho-H phenyls), 8.17 (8H, meta-H phenyls), 8.78 (H, pyrrole β-H). IR: ν (cm^{-1}) 1755, 1502, 1168, 1134, 1100, 964, 802.

Synthesis of Polystyrene Stars, $TPP(PS)_4$. The procedure used for synthesizing polystyrene stars, $TPP(PS)_4$, is as follows. ATRP of styrene was performed with a ratio of St/TPPBr/CuBr/PMEDTA = 400/1/4/8. A 50 mL Schlenk flask was charged with TPPBr (0.04 mmol, 50.0 mg), CuBr (0.16 mmol, 23.0 mg), and styrene (0.16 mol, 1.8 mL) under a nitrogen atmosphere. The solution was degassed by three freeze−pump−thaw cycles. Then anisole (2 mL) and PMDETA (0.32 mmol, 78 μL) were added, and another two freeze−pump−thaw cycles were performed. The polymerization was allowed to proceed at a preheated 90 °C oil bath. After that, the flask was quenched in liquid nitrogen to stop the polymerization. Then the reaction mixture was precipitated by pouring the solution into methanol followed by filtration and washing to yield $TPP(PS)_4$. The reaction time ranged from 2 to 4 h, and

dx.doi.org/10.1021/jp311439p | J. Phys. Chem. C 2013, 117, 6185−6194

the details of the stars were summarized in Table 1. ^{1}H NMR (500 MHz, $CDCl_3$): δ (ppm) 6.2−7.26 (5H, C_6H_5), 2.2−0.6 (3H, CH_2CH). IR: ν (cm^{-1}) 1755, 1600, 1494, 1449, 1195, 1161, 1100, 1009, 903, 756, 698.

Table 1. Results for the Synthesis of TPP(PS)$_4$

run	time (h)[a]	conv. (%)[b]	$M_{n,th}$[c]	$M_{n,GPC}$[d]	M_w/M_n[d]
1	2.0	23.8	11200	10300	1.25
2	2.5	30.7	14100	15300	1.37
3	3.0	36.8	16800	17800	1.42
4	4.5	42.1	19300	25600	1.84

[a][TPPBr]:[St]:[CuBr]:[PMDETA] = 1:400:4:10, [TPPBr] = 3.90 × 10^{-5} M, polymerization time varies from 2.0 to 4.5 h. [b]Calculated by the gravimetric method. Conv. (%) = W_p/W_{St}, where W_p and W_{St} are weights of the resultant polymer and styrene in feed, respectively. [c]Theoretical number-average molecular weight, $M_{n,th}$, was calculated according to $M_{n,th}$ = [St] × M_{St} × Conv./[TPPBr] + M_{TPPBr}. [d]Determined by GPC.

Hydrolysis of Polystyrene Stars, TPP(PS)$_4$. The star, 50 mg of TPP(PS)$_4$, was dissolved in 5 mL of THF in a 50 mL round-bottomed flask with KOH (1 g, 18 mmol) dissolved in 2 mL of water/ethanol mixture (1/1, v/v). The mixed solution was refluxed for 16 h and was then precipitated in methanol, centrifugated, dissolved in THF, precipitated in ethanol, and centrifugated. The product was successively washed with water/ethanol mixture (1:1, v/v) and absolute alcohol and dried in a vacuum oven overnight to achieve the final product, linear PS.

Synthesis of Block Stars, TPP(PS-*b*-PHEMA)$_4$. TPP(PS-*b*-PHEMA)$_4$ was synthesized using TPP(PS)$_4$ (M_n = 15300 g/mol) as a macroinitiator by ATRP with a ratio of HEMA/TPP(PS)$_4$/CuBr/PMEDTA = 20/1/4/8. A 50 mL Schlenk flask was charged with HEMA (0.2 mmol, 24 μL), TPP(PS)$_4$ (0.01 mmol, 153 mg), PMDETA (0.08 mmol, 17.6 μL), and chlorobenzene (5 mL) under a nitrogen atmosphere. The solution was degassed by three freeze−pump−thaw cycles. During the final cycle, CuBr (0.04 mmol, 5.7 mg) was added and followed by another three freeze−pump−thaw cycles. The reaction was allowed to proceed at a preheated 80 °C oil bath for 8 h. The reacting solution was exposed to the air to terminate the polymerization. THF was added to the reaction mixture, and the resulting solution was precipitated by pouring into petroleum ether. After centrifugation TPP(PS_{37}-*b*-$PHEMA_{1.4}$)$_4$ was obtained. TPP(PS_{37}-*b*-$PHEMA_7$)$_4$ was prepared according to the above-mentioned procedure but with a ratio of HEMA/TPP(PS)$_4$/CuBr/PMEDTA = 60/1/4/8. ^{1}H NMR (500 MHz, $CDCl_3$): δ (ppm) 6.2−7.26, (5H, C_6H_5), 2.2−0.6 (3H, CH_2CH), 4.32 (H, OH), 4.13 (2H, CH_2 bonded to ester group), 3.86 (2H, CH_2 bonded to hydroxyl group). IR: ν (cm^{-1}) 1755, 1726, 1600, 1494, 1449, 1195, 1164, 1100, 1024, 903, 756, 698.

Formation of Honeycomb Films via the Breath Figure Method. The films were cast by the breath figure method. The apparatus and procedure have been described in our previous work.[43] Poly(ethylene terephthalate) (PET) film was kindly provided by Hangzhou Tape Factory and cleaned with acetone for 2 h before use. TPP(PS)$_4$ and TPP(PS_{37}-*b*-$PHEMA_{1.4}$)$_4$ were dissolved in carbon disulfide at different concentrations. An aliquot of 50 μL for each polymer solution was drop-cast onto a PET substrate placed under a 2 L/min humid airflow (25 °C and ∼80% RH). Owing to the condensation of water vapor on the solution surface during the evaporation of carbon disulfide, the transparent solution soon turned turbid. After solidification, the film was dried at room temperature.

In Situ Observation of the Breath Figure Process. In situ observation of the film formation process was performed under an optical microscope equipped with a digital camera at a magnification of 160. Polymer solutions were cast on PET films fixed on the microscope table under a humid air flow. Videos started about 2 s before the solution was dropped and spread on the substrate and recorded through the solution hardening. Differences in factors such as air flow rate and the amount of polymer solution and its spreading may result in different hardening time. However, videos collected under different conditions showed the same trend. We repeated this more than 5 times for each sample, and the typical videos are presented (Supporting Information).

RESULTS AND DISCUSSION

Star polymers, polystyrene [TPP(PS)$_4$] and poly(styrene-*block*-2-hydroxyethyl methacrylate) [TPP(PS-*b*-PHEMA)$_4$], were synthesized by the "core-first" method through atom transfer radical polymerization (ATRP)[42,44] and employed for film preparation (Scheme 1). A tetrafunctional porphyrin initiator, $TPPBr_4$, was synthesized by reacting *meso*-tetrakis(4-hydroxylphenyl) porphyrin with 2-bromoisobutyryl bromide and then used for ATRP of styrene as well as the following chain extension. UV−vis absorption spectra strongly indicate that all of the four compounds display a typical Soret band of porphyrin near 420 nm (Figure 1). The fluorescence spectra show slight shifts because of the electronic effects of groups or chain blocks on the porphyrin core.[45,46] For example, a blue shift was observed after bromination of THPP, which is due to the introduction of an electron-withdrawing group.[45] The initiator and stars were also characterized by ^{1}H NMR (Figure

Scheme 1. Star Polymers Used for Preparing Honeycomb Films by the Breath Figure Method

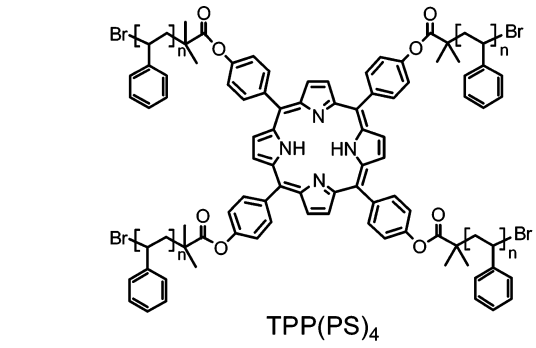

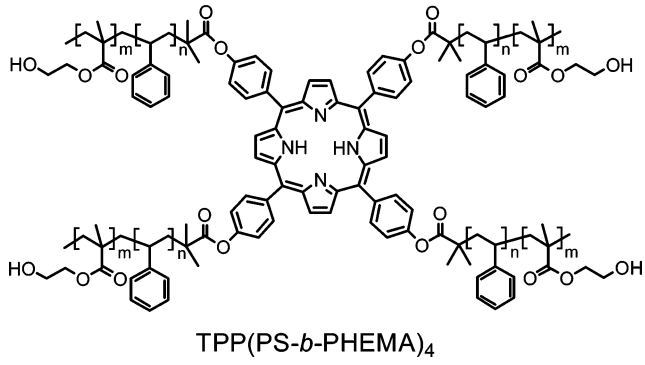

dx.doi.org/10.1021/jp311439p | J. Phys. Chem. C 2013, 117, 6185−6194

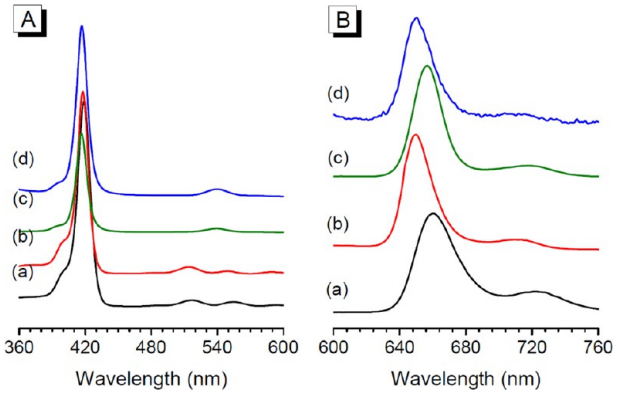

Figure 1. (A) UV and (B) fluorescence spectra of (a) THPP, (b) TPPBr, (c) $TPP(PS)_4$, and (d) $TPP(PS_{37}\text{-}b\text{-}PHEMA_{1.4})_4$. Excited at 420 nm.

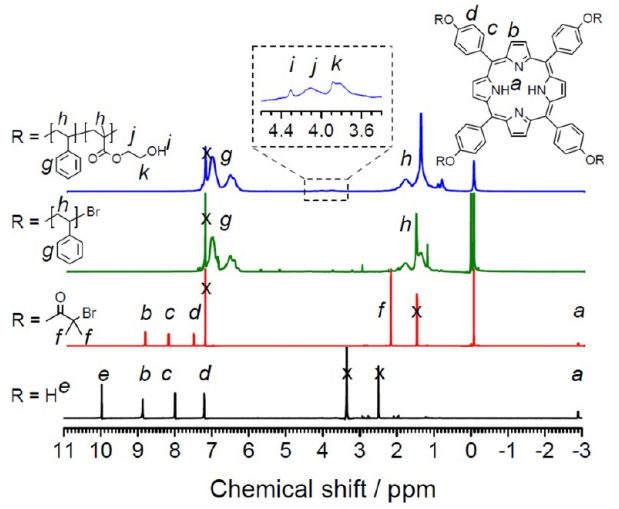

Figure 2. ^{1}H NMR spectra of THPP, TPPBr, $TPP(PS)_4$, and $TPP(PS_{37}\text{-}b\text{-}PHEMA_{1.4})_4$ (from bottom to top). The polymerization degree of the HEMA unit was estimated based on its characteristic peaks *i,j,k* and the GPC results of $TPP(PS)_4$.

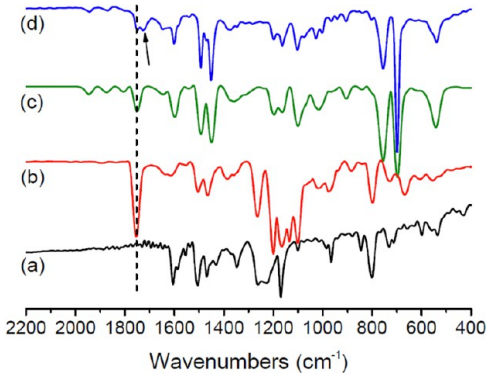

Figure 3. FTIR spectra of (a) THPP, (b) TPPBr, (c) $TPP(PS)_4$, and (d) $TPP(PS\text{-}b\text{-}PHEMA)_4$. The arrow shows the characteristic peak of C═O vibration of the ester carbonyl group of HEMA.

2) and FTIR (Figure 3). From the spectra of ^{1}H NMR, we can see the proton peak of the benzene ring between 6.2 and 7.3 after polymerization with styrene, and after being copolymerized with HEMA, the characteristic peaks of the HEMA unit appear between 3.6 and 4.4. The FTIR spectra further confirm the star polymers. The detailed characteristic peaks are summarized in the Experimental Methods section.

A coupling reaction may take place in the synthesis of multiarmed star polymers by the "core-first" strategy.[47,48] To obtain stars with definite structures, the reaction proceeded for only 2.5 h with a relatively low monomer conversion of 30.7% to avoid serious coupling reaction (Table 1), as indicated by GPC traces (Figure 4). Hydrolysis of the ester group that connects the polystyrene chain with the porphyrin core also elucidates that the ratios of the molecular weight of stars to that of one arm are close to 4 (Figure 4), which confirms the four-arm star polymers. It also means that the shoulder peaks should be attributed to the coupling reaction during the polymerization, not stars with two arms or three arms. We would like to point out that, although sometimes there are errors with the molecular weight of the star determined by GPC using linear PS calibration, MALDI-TOF experiments suggested that GPC is quite accurate.[42] Generally the hydrodynamic properties of PS stars of sufficient PS chain length should not be significantly different from linear PS. $TPP(PS_{37})_4$ with a molecular weight of 15 300 g/mol was used for chain extension to obtain block stars. The polymerization degrees of the HEMA unit were estimated as 1.4 and 7.0.

The process for preparing honeycomb films has been described in our previous work.[6,11] Briefly, the star polymer was dissolved in CS_2 at different concentrations. An aliquot of 50 μL for each polymer solution was drop-cast onto a poly(ethylene terephthalate) (PET) film. Then the film was immediately placed under a 2 L/min humid airflow (25 °C and ~80% RH). The transparent solution soon turned turbid. Widawski and co-workers[3] first reported honeycomb films from a star polymer because its high chain density and fast precipitation[33,39] can stabilize condensed water droplets to prevent the water droplets from coalescence. Figure 5 shows typical scanning electron microscope (SEM) and atomic force microscope (AFM) images of films fabricated from $TPP(PS)_4$ and $TPP(PS_{37}\text{-}b\text{-}PHEMA_{1.4})_4$ solutions at a concentration of 5 mg/mL. It should be noted that it is difficult to assess the accurate pore depth by AFM profile, but the results are helpful in comparing the two samples. It is remarkable that the pore diameter decreases from about 1 μm for $TPP(PS)_4$ film to about 240 nm for $TPP(PS_{37}\text{-}b\text{-}PHEMA_{1.4})_4$, and the pore depth declines from about 1.5 μm to about 100 nm accordingly. It is interesting that a slight difference in polymer structure leads to greatly different films. We envisaged that the change in pore diameter is attributed to the transition of monolayer into multilayer structures.

The multilayer array of pores is induced by the thermocapillary effect and Marangoni convection. First, water droplets condense on the surface of the polymer solution, forming the first layer of water droplets. Second, the water droplets are dragged into the polymer solution through a thermocapillary effect, and then the second water droplets are formed continuously on the surface of the polymer solution.[33] This process can repeat to form multilayer structure until the solvent is thoroughly evaporated.

The first thing we thought about is the interfacial tension. The distribution of the water drops inside the film and their stabilization are of prime importance, and hence the interfacial tension must be an important parameter. Fukuhira et al. investigated the effects of interfacial tension on film formation in solutions with surfactants.[49] Previously we also found that interfacial tension greatly affects the pore shape of honeycomb

dx.doi.org/10.1021/jp311439p | J. Phys. Chem. C 2013, 117, 6185−6194

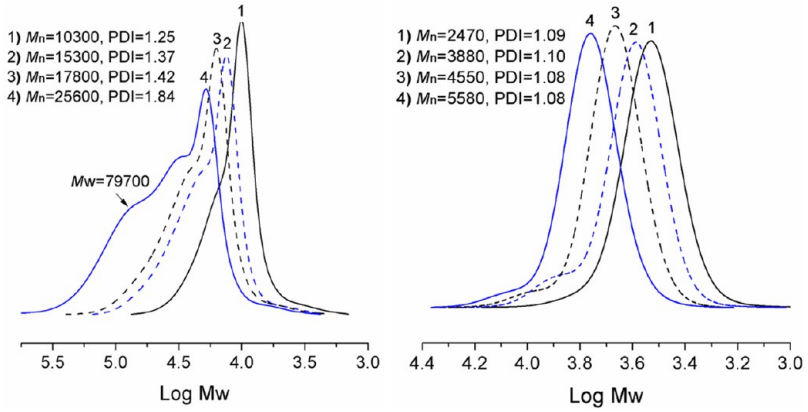

Figure 4. GPC curves of $TPP(PS)_4$ polymerized with different time (left) and PS hydrolyzed from the $TPP(PS)_4$ (right).

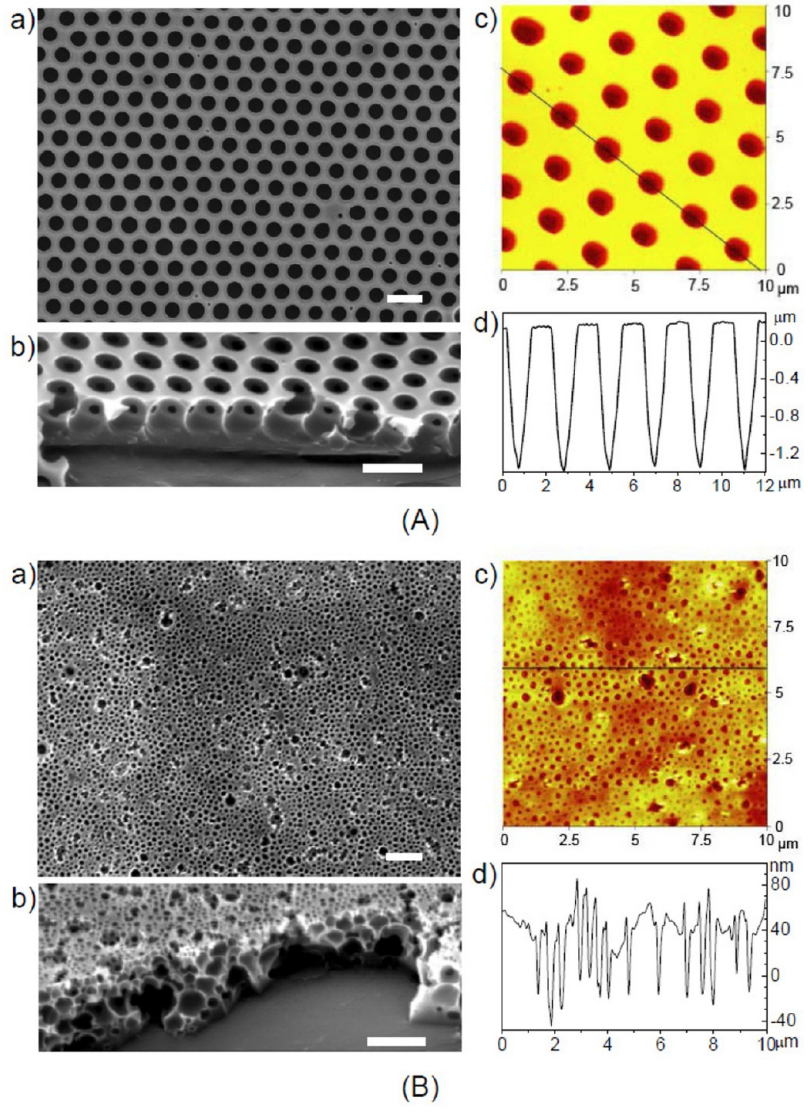

Figure 5. Morphology of honeycomb films prepared from (A) $TPP(PS)_4$ and (B) $TPP(PS_{37}$-*b*-$PHEMA_{1.4})_4$ solutions with a concentration of 5 mg/mL. (a) Surface and (b) cross-section SEM images; (c) AFM image; (d) depth profiles from the AFM image. Scale bars are 5 μm.

films.[43] However, one may not observe obvious differences in surface tension for these two star polymers as the structure difference is too small.

To facilitate the formation of multilayer structures, there are at least two pathways. One is to prolong the time of solution hardening. We traced the solidifying process of the star solutions under an optical microscope equipped with a digital camera. Videos started when the solution was dropped and spread on the substrate and were recorded until the solution had solidified. Typical images are shown in Figure 6. In a typical

dx.doi.org/10.1021/jp311439p | J. Phys. Chem. C 2013, 117, 6185−6194

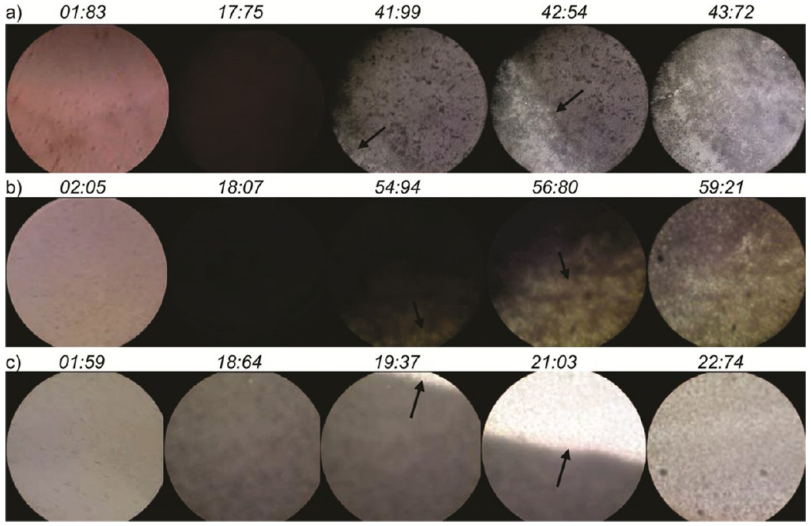

Figure 6. In situ observation of the breath figure process, which lasts less than 60 s. (a) 5 mg/mL of TPP(PS)$_4$, (b) 5 mg/mL of TPP(PS$_{37}$-*b*-PHEMA$_{1.4}$)$_4$, and (c) 1 mg/mL of TPP(PS$_{37}$-*b*-PHEMA$_{1.4}$)$_4$. The arrows denote the frontier of solidifying solutions (time scale: seconds).

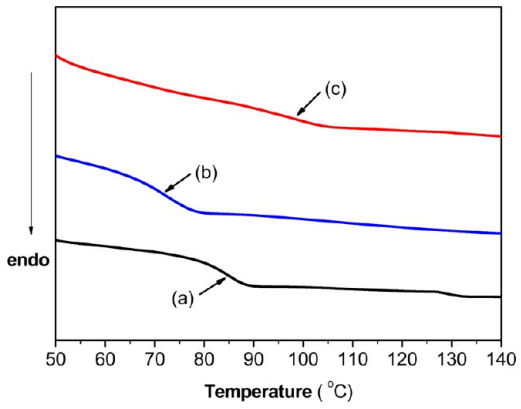

Figure 7. DSC curves of (a) TPP(PS)$_4$, (b) TPP(PS$_{37}$-*b*-PHEMA$_{1.4}$)$_4$, and (c) TPP(PS$_{37}$-b-PHEMA$_{7.0}$)$_4$, the glass transition temperatures of which are 85 °C, 72 °C, and 98 °C, respectively.

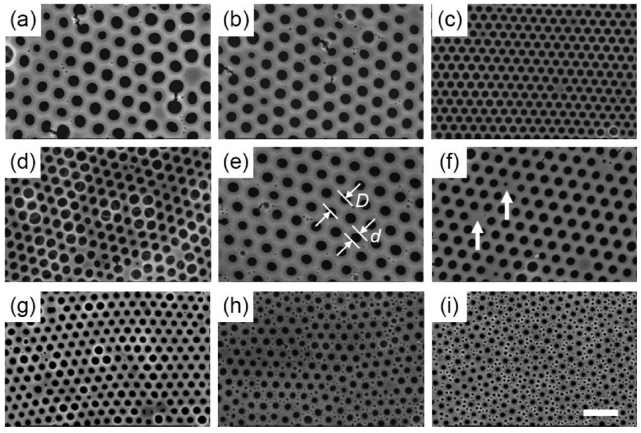

Figure 8. (a–i) SEM images of films prepared from TPP(PS)$_4$ solutions of 3–11 mg/mL. The films were prepared from the CS_2 solutions under 2 L/min airflow. Scale bar is 5 μm.

experiment, the solidifying of TPP(PS)$_4$ solution occurs at the 42nd second (the field of microscope changes from dark to bright, see Figure 6a), whereas TPP(PS$_{37}$-*b*-PHEMA$_{1.4}$)$_4$ solution starts at the 55th second (Figure 6b). Longer solution solidifying time makes it continuously repeatable for the water droplets to condense, grow, and submerge.

Fast precipitation of star polymers is also necessary for multilayer structures with small stabilized water droplets by shortening their growth time. It is difficult to directly observe the precipitation of polymers during the breath figure process. We evaluated the segmental motion of polymer chains by measuring the glass transition temperature (T_g) using a differential scanning calorimeter (DSC). As shown in Figure 7, the T_g of TPP(PS)$_4$ is 85 °C, which is lower than the classical value around 100 °C for high molecular weight polystyrene. This decrease should be related to both the star structure that has more end groups and the low molecular weight of the star polymer, as the shorter the chains, the lower the T_g value is.[50] The T_g of the star polymer TPP(PS$_{37}$-*b*-PHEMA$_{1.4}$)$_4$ further decreases to 72 °C, which is caused by the end groups that increase the free volume of the polymer especially for a polymer with low molecular weight.[51] Its lower T_g of TPP(PS$_{37}$-*b*-PHEMA$_{1.4}$)$_4$ suggests probably easier segmental motion and faster precipitation at the interface between polymer solution and water droplets. For the star copolymer with longer PHEMA block length of 7.0, the T_g increases to 98 °C, which is attributed to the hydrogen bonding interactions in PHEMA chain segments. It should be noted that TPP(PS$_{37}$-*b*-PHEMA$_{7.0}$)$_4$ cannot dissolve in nonpolar CS_2 for film formation.

In addition, from the in situ video (Supporting Information) we can observe a very dark period during the film formation process for TPP(PS$_{37}$-*b*-PHEMA$_{1.4}$)$_4$, which lasts from the 15th second through solution solidifying. This dark period, which is much longer than that of TPP(PS)$_4$, reveals the formation of a multilayer structure. It is speculated that the breath figure process can be roughly divided into three stages. In the first stage, the solution is homogeneous and transparent under the microscopy. Then, a large number of water droplets condense onto/into the solution and the solution becomes opaque. Finally, solvent evaporates thoroughly, leading to a very thin cured film that is transparent again. The second period for the two polymers is significantly different because of the formation of mono- or multilayer structure. Overall, fast precipitation of polymers in a delayed solidifying solution prefers multilayer

dx.doi.org/10.1021/jp311439p | J. Phys. Chem. C 2013, 117, 6185–6194

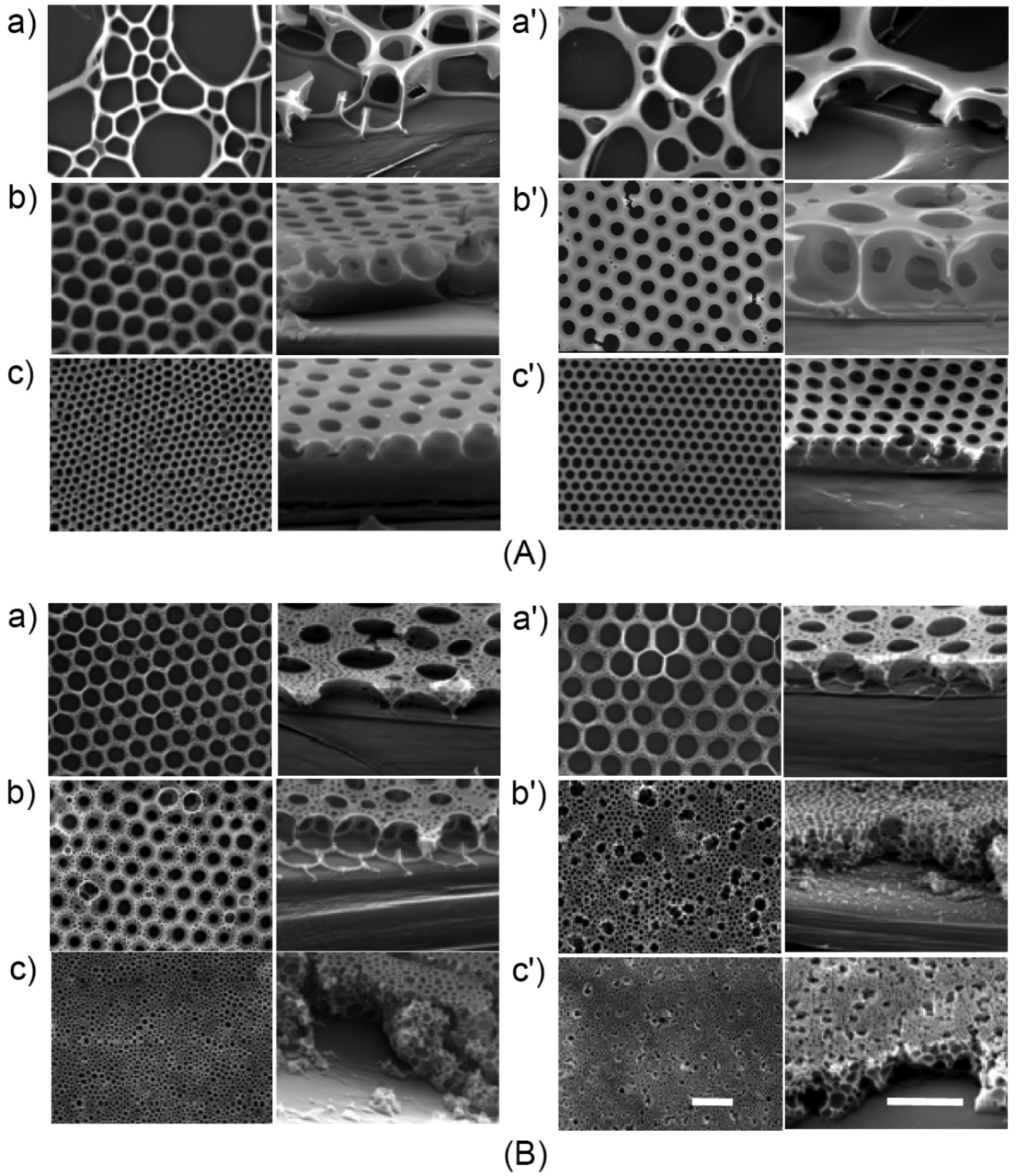

Figure 9. Top-down and cross-sectional SEM images of (A) TPP$(PS)_4$ and (B) TPP$(PS_{37}$-b-$PHEMA_{1.4})_4$ films. (a,b,c) Edge area. (a′,b′,c′) Center area of films. Polymer concentration: (a,a′) 1 mg/mL; (b,b′) 3 mg/mL; (c,c′) 5 mg/mL. Scale bars are 5 μm. The cross-section images were taken at higher magnification.

structure, lowers the growth time of water droplets at every layer especially at the top layer, and hence decreases the pore size to submicrometer scale.

The precipitation of star polymers also shows important effects on the pore size of TPP$(PS)_4$ film. Figure 8 displays SEM images of films cast from solutions of TPP$(PS)_4$ with different concentrations. In the range of 3−11 mg/mL, hexagonally packed films are formed. However, the dependence of pore diameter (d) or pore distance (D) on the concentration of the star polymer does not show pronounced tendency, which is similar to comb-like copolymers but different from most amphiphilic linear copolymers.[33,52] For amphiphilic copolymers that show surfactant-like interfacial activity, a larger amount of polymer can thermodynamically stabilize larger interfacial area, leading to smaller pore size. However, the star polystyrene affects pore size mainly through the rate of precipitation around water droplets, which almost does not depend on polymer concentration.

The pore structure in the edge area of the TPP$(PS)_4$ films is similar to that in the center area; i.e., they are monolayer and have almost the same pore size (in some cases the size of pores in the center area is slightly larger because of longer growth time, Figure 9A). It has been suggested that the polymer with hydrophilic moieties can form regular patterns at lower concentration than the hydrophobic polymer due to the easier gathering of hydrophilic polymer molecules on the solution surface.[53] Similarly, we obtained hexagonal honeycomb films using TPP$(PS_{37}$-b-$PHEMA_{1.4})_4$ solution with a concentration of 1 mg/mL (Figure 9B); however, at this concentration an irregular network was formed for TPP$(PS)_4$. At the

dx.doi.org/10.1021/jp311439p | J. Phys. Chem. C 2013, 117, 6185−6194

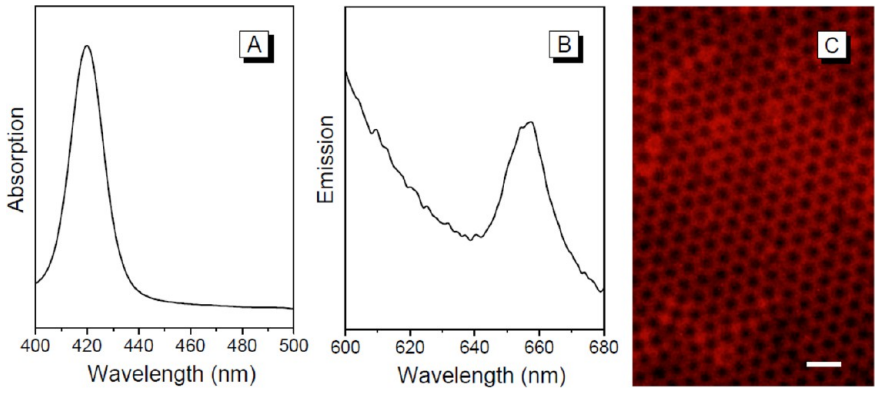

Figure 10. (A) UV, (B) fluorescence spectra (excited at 380 nm), and (C) fluorescence microscopy image of honeycomb porous TPP(PS)$_4$ film. Scale bar is 5 μm.

concentration of 1 mg/mL, both the edge area and center area of TPP(PS$_{37}$-*b*-PHEMA$_{1.4}$)$_4$ film have monolayer structure. The in situ video shows that the hardening time of 1 mg/mL of TPP(PS$_{37}$-*b*-PHEMA$_{1.4}$)$_4$ solution starts at the 20th second (Figure 6c), which is about 35 s faster than that of 5 mg/mL solution. A solution of 3 mg/mL generates monolayer edge area but multilayer center area. However, a homogeneous film with multilayer structure can be obtained at a concentration of 5 mg/mL. The difference in the edge and center areas arises from thinner solution[54] and larger evaporative flux[55] at the edge area. These two factors result in smaller pores in the edge area.[17] This dependence of mono- or multilayer structures on polymer concentration is consistent with the literature.[33,56]

It can be seen from the UV and fluorescence spectra that the honeycomb films still maintain the photophysical properties of porphyrin (Figure 10). Fluorescence microscopy image also confirms the fluorescence characteristic of the porphyrin materials. It should be noted that the hexagonal patterns may be distorted to some extent with the decrease of pore size. However, for some applications high levels of ordering may not be so vital, and the pore-size range of 200−500 nm is potentially interesting for membrane preparation.

CONCLUSIONS

In conclusion, we have proposed a novel strategy for the fabrication of honeycomb films with homogeneous submicrometer-sized pores. Well-defined star polymers TPP(PS)$_4$ and TPP(PS-*b*-PHEMA)$_4$, which were synthesized by ATRP using tetrafunctional porphyrin as the core, were utilized to fabricate honeycomb films by the breath figure method. The pore size can be dramatically lowered to about 240 nm for TPP(PS-*b*-PHEMA)$_4$ compared with that of TPP(PS)$_4$ which is about 1 μm. TPP(PS-*b*-PHEMA)$_4$ only contains a small amount of HEMA units but is greatly different from TPP(PS)$_4$. The former results in multilayer structure, whereas the latter generates monolayers. This difference in the film structures can be attributed to both longer hardening time of solutions and faster precipitation rate of polymers. The proposed strategy for films with submicrometer-sized pores is useful in preparing advanced microfiltration membranes.

ASSOCIATED CONTENT

Supporting Information

In situ videos for films prepared from 5 mg/mL of TPP(PS)$_4$ solution (jp311439p_si_001.mpg), 5 mg/mL of TPP(PS$_{37}$-*b*-PHEMA$_{1.4}$)$_4$ solution (jp311439p_si_002.mpg), and 1 mg/mL of TPP(PS$_{37}$-*b*-PHEMA$_{1.4}$)$_4$ solution (jp311439p_si_003.mpg). This material is available free of charge via the Internet at http://pubs.acs.org.

AUTHOR INFORMATION

Corresponding Author

*Tel.: +86-571-87953763. E-mail: lswan@zju.edu.cn.

Notes

The authors declare no competing financial interest.

ACKNOWLEDGMENTS

This work was supported by the National Natural Science Foundation of China (51173161) and partially supported by the Zhejiang Provincial Natural Science Foundation of China (Y4110076) and the Program for Zhejiang Provincial Innovative Research Team (2009R50004). We appreciate Prof. Jian Wu and Mr. Fu-Wen Lin at the Department of Chemistry, Zhejiang University, for the help in the synthesis of THPP.

REFERENCES

(1) Sumper, M. A Phase Separation Model for the Nanopatterning of Diatom Biosilica. *Science* **2002**, *295*, 2430−2433.
(2) Xia, Y.; Whitesides, G. M. Soft Lithography. *Angew. Chem., Int. Ed.* **1998**, *37*, 550−575.
(3) Widawski, G.; Rawiso, M.; Francois, B. Self-Organized Honeycomb Morphology of Star-Polymer Polystyrene Films. *Nature* **1994**, *369*, 387−389.
(4) Zhang, Y.; Wang, C. Micropatterning of Proteins on 3D Porous Polymer Films Fabricated by Using the Breath-Figure Method. *Adv. Mater.* **2007**, *19*, 913−916.
(5) Min, E.; Wong, K. H.; Stenzel, M. H. Microwells with Patterned Proteins by a Self-Assembly Process Using Honeycomb-Structured Porous Films. *Adv. Mater.* **2008**, *20*, 3550−3556.
(6) Ke, B. B.; Wan, L. S.; Xu, Z. K. Controllable Construction of Carbohydrate Microarrays by Site-Directed Grafting on Self-Organized Porous Films. *Langmuir* **2010**, *26*, 8946−8952.
(7) Wan, L. S.; Li, Q. L.; Chen, P. C.; Xu, Z. K. Patterned Biocatalytic Films Via One-Step Self-Assembly. *Chem. Commun.* **2012**, *48*, 4417−4419.
(8) Boker, A.; Lin, Y.; Chiapperini, K.; Horowitz, R.; Thompson, M.; Carreon, V.; Xu, T.; Abetz, C.; Skaff, H.; Dinsmore, A. D.; Emrick, T.; Russell, T. P. Hierarchical Nanoparticle Assemblies Formed by Decorating Breath Figures. *Nat. Mater.* **2004**, *3*, 302−306.
(9) Sun, H.; Li, H. L.; Bu, W. F.; Xu, M.; Wu, L. X. Self-Organized Microporous Structures Based on Surfactant-Encapsulated Polyoxometalate Complexes. *J. Phys. Chem. B* **2006**, *110*, 24847−24854.

(10) Sun, W.; Ji, J.; Shen, J. C. Rings of Nanoparticle-Decorated Honeycomb-Structured Polymeric Film: The Combination of Pickering Emulsions and Capillary Flow in the Breath Figures Method. *Langmuir* **2008**, *24*, 11338−11341.
(11) Ke, B. B.; Wan, L. S.; Chen, P. C.; Zhang, L. Y.; Xu, Z. K. Tunable Assembly of Nanoparticles on Patterned Porous Film. *Langmuir* **2010**, *26*, 15982−15988.
(12) Ma, H. M.; Hao, J. C. Evaporation-Induced Ordered Honeycomb Structures of Gold Nanoparticles at the Air/Water Interface. *Chem.—Eur. J.* **2010**, *16*, 655−660.
(13) Ma, C. Y.; Zhong, Y. W.; Li, J.; Chen, C. K.; Gong, J. L.; Xie, S. Y.; Li, L.; Ma, Z. Patterned Carbon Nanotubes with Adjustable Array: A Functional Breath Figure Approach. *Chem. Mater.* **2010**, *22*, 2367−2374.
(14) Jiang, X. L.; Zhou, X. F.; Zhang, Y.; Zhang, T. Z.; Guo, Z. R.; Gu, N. Interfacial Effects of in Situ-Synthesized Ag Nanoparticles on Breath Figures. *Langmuir* **2010**, *26*, 2477−2483.
(15) Li, L.; Zhong, Y. W.; Ma, C. Y.; Li, J.; Chen, C. K.; Zhang, A. J.; Tang, D. L.; Xie, S. Y.; Ma, Z. Honeycomb-Patterned Hybrid Films and Their Template Applications Via a Tunable Amphiphilic Block Polymer/Inorganic Precursor System. *Chem. Mater.* **2009**, *21*, 4977−4983.
(16) Galeotti, F.; Andicsova, A.; Yunus, S.; Botta, C. Precise Surface Patterning of Silk Fibroin Films by Breath Figures. *Soft Matter* **2012**, *8*, 4815−4821.
(17) Yabu, H.; Shimomura, M. Single-Step Fabrication of Transparent Superhydrophobic Porous Polymer Films. *Chem. Mater.* **2005**, *17*, 5231−5234.
(18) Nishikawa, T.; Nishida, J.; Ookura, R.; Nishimura, S. I.; Wada, S.; Karino, T.; Shimomura, M. Honeycomb-Patterned Thin Films of Amphiphilic Polymers as Cell Culture Substrates. *Mater. Sci. Eng., C: Biomimetic Supramol. Syst.* **1999**, *8*−*9*, 495−500.
(19) Zhu, Y. D.; Sheng, R. L.; Luo, T.; Li, H.; Sun, J. J.; Chen, S. D.; Sun, W. Y.; Cao, A. M. Honeycomb-Structured Films by Multifunctional Amphiphilic Biodegradable Copolymers: Surface Morphology Control and Biomedical Application as Scaffolds for Cell Growth. *ACS Appl. Mater. Interfaces* **2011**, *3*, 2487−2495.
(20) Du, M. C.; Zhu, P. L.; Yan, X. H.; Su, Y.; Song, W. X.; Li, J. B. Honeycomb Self-Assembled Peptide Scaffolds by the Breath Figure Method. *Chem.—Eur. J.* **2011**, *17*, 4238−4245.
(21) Chen, J. J.; Ho, Q. P.; Wang, M. J. Modulation of Cell Responses by Creating Surface Submicron Topography and Amine Functionalities. *J. Polym. Sci., Part B: Polym. Phys.* **2012**, *50*, 484−491.
(22) Chen, P. C.; Wan, L. S.; Ke, B. B.; Xu, Z. K. Honeycomb-Patterned Film Segregated with Phenylboronic Acid for Glucose Sensing. *Langmuir* **2011**, *27*, 12597−12605.
(23) Liu, C. H.; Gao, C.; Yan, D. Y. Honeycomb-Patterned Photoluminescent Films Fabricated by Self-Assembly of Hyperbranched Polymers. *Angew. Chem., Int. Ed.* **2007**, *46*, 4128−4131.
(24) Lee, S. H.; Kim, H. W.; Hwang, J. O.; Lee, W. J.; Kwon, J.; Bielawski, C. W.; Ruoff, R. S.; Kim, S. O. Three-Dimensional Self-Assembly of Graphene Oxide Platelets into Mechanically Flexible Macroporous Carbon Films. *Angew. Chem., Int. Ed.* **2010**, *49*, 10084−10088.
(25) Wang, J.; Wang, C. F.; Shen, H. X.; Chen, S. Quantum-Dot-Embedded Ionomer-Derived Films with Ordered Honeycomb Structures Via Breath Figures. *Chem. Commun.* **2010**, *46*, 7376−7378.
(26) Yin, S. Y.; Zhang, Y. Y.; Kong, J. H.; Zou, C. J.; Li, C. M.; Lu, X. H.; Ma, J.; Boey, F. Y. C.; Chen, X. D. Assembly of Graphene Sheets into Hierarchical Structures for High-Performance Energy Storage. *ACS Nano* **2011**, *5*, 3831−3838.
(27) Wang, J.; Shen, H. X.; Wang, C. F.; Chen, S. Multifunctional Ionomer-Derived Honeycomb-Patterned Architectures and Their Performance in Light Enhancement of Light-Emitting Diodes. *J. Mater. Chem.* **2012**, *22*, 4089−4096.
(28) Heng, L. P.; Qin, W.; Chen, S. J.; Hu, R. R.; Li, J.; Zhao, N.; Wang, S. T.; Tang, B. Z.; Jiang, L. Fabrication of Small Organic Luminogens Honeycomb-Structured Films with Aggregation-Induced Emission Features. *J. Mater. Chem.* **2012**, *22*, 15869−15873.
(29) Erdogan, B.; Song, L. L.; Wilson, J. N.; Park, J. O.; Srinivasarao, M.; Bunz, U. H. F. Permanent Bubble Arrays from a Cross-Linked Poly(Para-Phenyleneethynylene): Picoliter Holes without Microfabrication. *J. Am. Chem. Soc.* **2004**, *126*, 3678−3679.
(30) Li, X. F.; Zhang, L. A.; Wang, Y. X.; Yang, X. L.; Zhao, N.; Zhang, X. L.; Xu, J. A Bottom-up Approach to Fabricate Patterned Surfaces with Asymmetrical TiO(2) Microparticles Trapped in the Holes of Honeycomblike Polymer Film. *J. Am. Chem. Soc.* **2011**, *133*, 3736−3739.
(31) Wan, L. S.; Li, J. W.; Ke, B. B.; Xu, Z. K. Ordered Microporous Membranes Templated by Breath Figures for Size-Selective Separation. *J. Am. Chem. Soc.* **2012**, *134*, 95−98.
(32) Cong, H.; Wang, J.; Yu, B.; Tang, J. Preparation of a Highly Permeable Ordered Porous Microfiltration Membrane of Brominated Poly(Phenylene Oxide) on an Ice Substrate by the Breath Figure Method. *Soft Matter* **2012**, *8*, 8835−8839.
(33) Stenzel, M. H.; Barner-Kowollik, C.; Davis, T. P. Formation of Honeycomb-Structured, Porous Films Via Breath Figures with Different Polymer Architectures. *J. Polym. Sci., Part A: Polym. Chem.* **2006**, *44*, 2363−2375.
(34) Kittel, C.; Kroemer, H. *Thermal Physics*; Freeman: New York, 1980.
(35) Bunz, U. H. F. Breath Figures as a Dynamic Templating Method for Polymers and Nanomaterials. *Adv. Mater.* **2006**, *18*, 973−989.
(36) Karikari, A. S.; Williams, S. R.; Heisey, C. L.; Rawlett, A. M.; Long, T. E. Porous Thin Films Based on Photo-Cross-Linked Star-Shaped Poly(D, L-Lactide)S. *Langmuir* **2006**, *22*, 9687−9693.
(37) Connal, L. A.; Vestberg, R.; Hawker, C. J.; Qiao, G. G. Dramatic Morphology Control in the Fabrication of Porous Polymer Films. *Adv. Funct. Mater.* **2008**, *18*, 3706−3714.
(38) Dong, W. Y.; Zhou, Y. F.; Yan, D. Y.; Mai, Y. Y.; He, L.; Jin, C. Y. Honeycomb-Structured Microporous Films Made from Hyperbranched Polymers by the Breath Figure Method. *Langmuir* **2009**, *25*, 173−178.
(39) Barner-Kowollik, C.; Dalton, H.; Davis, T. P.; Stenzel, M. H. Nano- and Micro-Engineering of Ordered Porous Blue-Light-Emitting Films by Templating Well-Defined Organic Polymers around Condensing Water Droplets. *Angew. Chem., Int. Ed.* **2003**, *42*, 3664−3668.
(40) Hernandez-Guerrero, M.; Davis, T. P.; Barner-Kowollik, C.; Stenzel, M. H. Polystyrene Comb Polymers Built on Cellulose or Poly(Styrene-Co-2-Hydroxyethylmethacrylate) Backbones as Substrates for the Preparation of Structured Honeycomb Films. *Eur. Polym. J.* **2005**, *41*, 2264−2277.
(41) Bolognesi, A.; Galeotti, F.; Moreau, J.; Giovanella, U.; Porzio, W.; Scavia, G.; Bertini, F. Unsoluble Ordered Polymeric Pattern by Breath Figure Approach. *J. Mater. Chem.* **2010**, *20*, 1483−1488.
(42) High, L. R. H.; Holder, S. J.; Penfold, H. V. Synthesis of Star Polymers of Styrene and Alkyl (Meth)Acrylates from a Porphyrin Initiator Core via ATRP. *Macromolecules* **2007**, *40*, 7157−7165.
(43) Wan, L. S.; Ke, B. B.; Zhang, J.; Xu, Z. K. Pore Shape of Honeycomb-Patterned Films: Modulation and Interfacial Behavior. *J. Phys. Chem. B* **2012**, *116*, 40−47.
(44) Matyjaszewski, K. The Synthesis of Functional Star Copolymers as an Illustration of the Importance of Controlling Polymer Structures in the Design of New Materials. *Polym. Int.* **2003**, *52*, 1559−1565.
(45) Aramata, K.; Kajiwara, A.; Hashidzume, A.; Morishima, Y.; Kamachi, M. Radical Polymerization of 5-(4′-Acrylamidophenyl)-10,15,20-triphenylporphine and 5-(4′-Methacrylamidophenyl)-10,15,20-triphenylporphine. *Polym. J.* **1998**, *30*, 702−707.
(46) Aramata, K.; Kamachi, M.; Takahashi, M.; Yamagishi, A. Orientation of Porphyrin Moieties in Langmuir-Blodgett Films of Tetraphenylporphyrin Vinyl Monomers and Their Polymers. *Langmuir* **1997**, *13*, 5161−5167.
(47) Zhao, Y. L.; Shuai, X. T.; Chen, C. F.; Xi, F. Synthesis of Star Block Copolymers from Dendrimer Initiators by Combining Ring-Opening Polymerization and Atom Transfer Radical Polymerization. *Macromolecules* **2004**, *37*, 8854−8862.

(48) Zhang, C. B.; Zhou, Y. A.; Liu, Q. A.; Li, S. X.; Perrier, S.; Zhao, Y. L. Facile Synthesis of Hyperbranched and Star-Shaped Polymers by Raft Polymerization Based on a Polymerizable Trithiocarbonate. *Macromolecules* **2011**, *44*, 2034−2049.
(49) Fukuhira, Y.; Yabu, H.; Ijiro, K.; Shimomura, M. Interfacial Tension Governs the Formation of Self-Organized Honeycomb-Patterned Polymer Films. *Soft Matter* **2009**, *5*, 2037−2041.
(50) Khalyavina, A.; Häußler, L.; Lederer, A. Effect of the Degree of Branching on the Glass Transition Temperature of Polyesters. *Polymer* **2012**, *53*, 1049−1053.
(51) Sinnwell, S.; Ritter, H. Microwave Accelerated Polymerization of 2-Phenyl-5,6-dihydro-4h-1,3-oxazine: Kinetics and Influence of End-Groups on Glass Transition Temperature. *Macromol. Rapid Commun.* **2006**, *27*, 1335−1340.
(52) Ke, B. B.; Wan, L. S.; Zhang, W. X.; Xu, Z. K. Controlled Synthesis of Linear and Comb-Like Glycopolymers for Preparation of Honeycomb-Patterned Films. *Polymer* **2010**, *51*, 2168−2176.
(53) Tian, Y.; Liu, S.; Ding, H. Y.; Wang, L. H.; Liu, B. Q.; Shi, Y. Q. Formation of Honeycomb-Patterned Polyetherketone Cardo (PEK-C) Films in a Highly Humid Atmosphere. *Macromol. Chem. Phys.* **2006**, *207*, 1998−2005.
(54) Hayakawa, T.; Horiuchi, S. From Angstroms to Micrometers: Self-Organized Hierarchical Structure within a Polymer Film. *Angew. Chem., Int. Ed.* **2003**, *42*, 2285−2289.
(55) Connal, L. A.; Gurr, P. A.; Qiao, G. G.; Solomon, D. H. From Well Defined Star-Microgels to Highly Ordered Honeycomb Films. *J. Mater. Chem.* **2005**, *15*, 1286−1292.
(56) Zhang, W. X.; Wan, L. S.; Meng, X. L.; Li, J. W.; Ke, B. B.; Chen, P. C.; Xu, Z. K. Macroporous, Protein-Containing Films Cast from Water-in-Oil Emulsions Featuring a Block-Copolymer. *Soft Matter* **2011**, *7*, 4221−4227.